

# Effects of Ionic Doping on the Behaviors of Oxygen Vacancies in HfO<sub>2</sub> and ZrO<sub>2</sub>: A First Principles Study

Haowei Zhang, Bin Gao, Shimeng Yu, Lin Lai<sup>†</sup>, Lang Zeng, Bing Sun, Lifeng Liu, Xiaoyan Liu, Jing Lu<sup>†</sup>, Ruqi Han, Jinfeng Kang,\*

Institute of Microelectronics, Peking University & Key Laboratory of Microelectronic Devices and Circuits, Ministry of Education, Beijing 100871, China, \*E-mail: kangjf@pku.edu.cn

<sup>†</sup>State Key Laboratory for Mesoscopic Physics and Department of Physics, Peking University, Beijing 100871, China

**Abstract**—The effects of metallic ion (Al, Ti, or La) doping in HfO<sub>2</sub> or ZrO<sub>2</sub> on the behaviors of oxygen vacancies ( $V_o$ ) such as the formation energy, density of states, and migration energy were investigated by using first principles calculations. The calculations show that, 1) the doping causes an upward shift of deep  $V_o$  levels; 2) dopant radius has a weak impact on the relaxed formation energy of  $V_o$  ( $E_f^v$ ) but a significant impact on the unrelaxed  $E_f^v$ ; 3) the relaxed formation energy  $E_f^v$  of  $V_o$  is remarkably reduced by trivalent ion (Al or La) doping compared to by tetravalent ion (Ti) doping; 4) Al, Ti, or La doping impacts the migration barriers of  $V_o$  along different directions.

**Keywords:** Hafnium Oxide, Zirconium Oxide, First Principles Calculation, Ionic Doping Effect, Oxygen Vacancy

## Introduction

Hf- or Zr-based oxides have been extensively studied for the application in advanced CMOS logic and memory devices [1-3]. It has been demonstrated that the critical device behaviors such as the reliability and work function tuning of high-k/metal gate stacks or the switching behaviors of metal-oxide based resistive random access memory (RRAM) are correlated with the intrinsic oxygen vacancies ( $V_o$ ) in HfO<sub>2</sub> or ZrO<sub>2</sub> [1-4]. Understanding the doping effects on the behaviors of  $V_o$  in HfO<sub>2</sub> and ZrO<sub>2</sub> may help to fundamentally understand the doping effect on the device behaviors, which is crucial for the applications of Hf- or Zr-based oxides in high-k/metal gate stacks and RRAM. In this paper, the behaviors of  $V_o$  such as the formation energy, density of state, and diffusivity in pure and Al-, Ti-, or La-doped HfO<sub>2</sub> and ZrO<sub>2</sub> were investigated based on the first principles calculations.

## Computational Methods

The density functional theory (DFT) calculations were carried out by using a generalized gradient approximation (GGA) for the exchange-correlation potential and Vanderbilt-

type ultrasoft pseudopotentials as implemented in the CASTEP code [5]. A supercell of monoclinic HfO<sub>2</sub> or ZrO<sub>2</sub> containing 96 atoms was constructed. The oxygen atoms in monoclinic HfO<sub>2</sub> or ZrO<sub>2</sub> are either threefold or fourfold coordinated, leading to two kinds of  $V_o$  configurations as shown in Fig. 1.

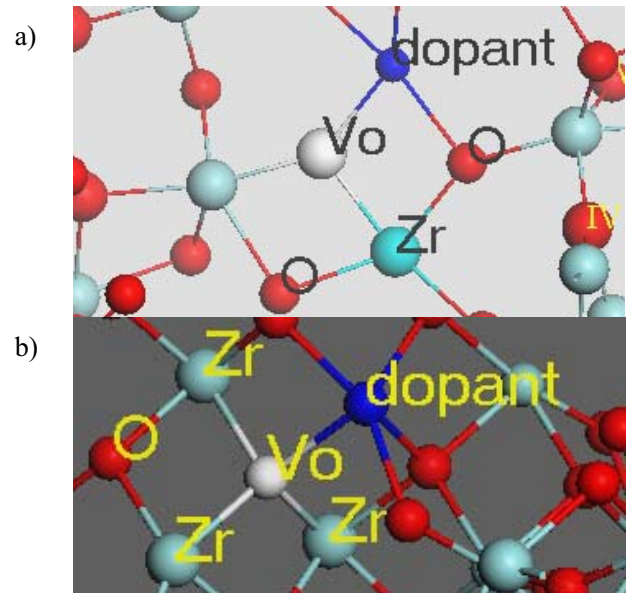


Fig1. Schematic views of three coordinated (a) and four coordinated (b) oxygen vacancy ( $V_o$ ) at nearest neighboring (NN) position to the dopant.

In the calculations, the  $V_o$  properties were simulated by removing one oxygen atom from the supercell and the doping effect was investigated by using a dopant to replace a Hf or Zr atom. Because threefold coordinated vacancy binding with dopant forms relatively stable configuration [6], this work focuses on the three coordinated vacancy. The geometry optimization was performed to relax atoms by fixing the total volume. The  $V_o$  formation energy is defined as

$$E_f^v = E_{vac} - E_{free} + \mu_O,$$

where  $E_{vac}$  and  $E_{free}$  denote the total energy of the supercell

with and without a  $V_O$  in the nearest neighbor (NN) of the dopant, respectively.  $\mu_O$  is the chemical potential of O, and it is half of the oxygen molecule energy in this calculation. The relaxed or unrelaxed  $V_O$  formation energy corresponds to the energy with or without lattice relaxation. To simulate the vacancy diffusion in  $ZrO_2$ , one oxygen ion is moved from the lattice site to the neighboring vacant sites.

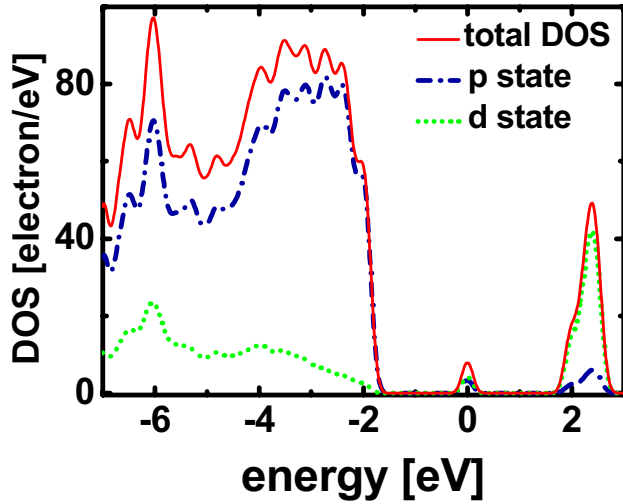


Fig2. Density of state (DOS) of  $HfO_2$  with  $V_O$ . The Fermi Level is at 0eV.

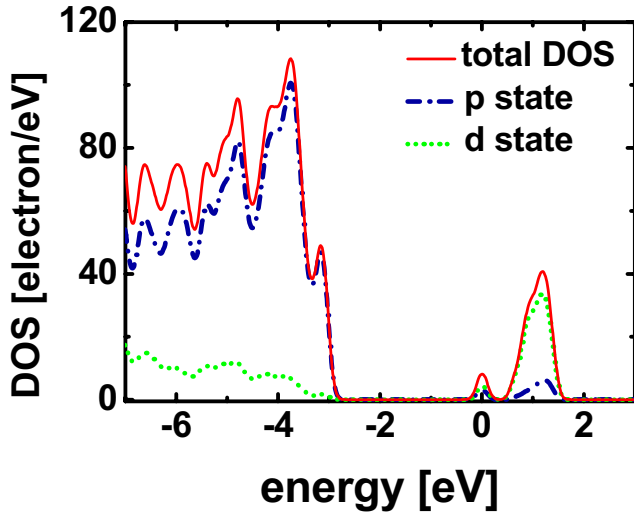


Fig3. DOS of Al doped  $HfO_2$  with  $V_O$  at the NN position to the dopant. The deep level is shifted upward, leading to shallow level.

The migration barrier ( $E_m$ ) is defined as the total energy difference between saddle point energy of the migration process and the energy of the  $V_O$  at the initial site [7]. Transition state search is used to calculate  $E_m$ . The electron wave functions are described within a plane-wave basis set with an energy cutoff of 300eV. Brillouin Zone (BZ) is

sampled at the  $\Gamma$  point. Geometry optimizations are performed until atomic forces are smaller than 0.03eV/Å. Linear Synchronous Transit (LST), followed by repeated conjugate gradient minimizations and Quadric Synchronous Transit (QST) maximizations calculations are performed to search the saddle point in the  $V_O$  migration process.

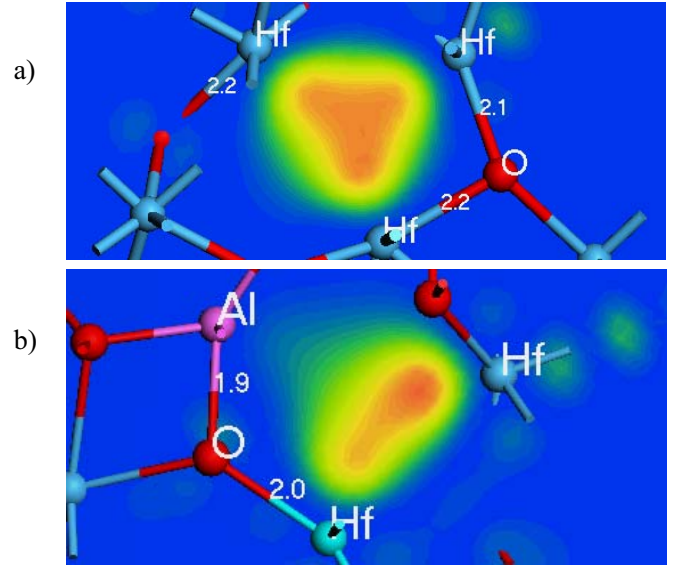


Fig4. Wave function contour plot corresponding to the gap-state at  $V_O$  site in undoped (a) and Al doped  $HfO_2$  (b). The localized gap state is mainly contributed from the d states of Hf.

## Results

Figure 2 shows the density of states (DOS) of  $HfO_2$  with  $V_O$ . The calculated band gap is about 3.3 eV, which is consistent with other DFT calculations [8, 9]. It should be noted that the calculated data is smaller than the experimental data of 5.68 eV [10] due to the well known band gap underestimations of DFT calculations [8]. Fermi level is at mid-gap state, indicating that the defect level of the neutrally charged  $V_O$  is occupied. Contour plot of wave function corresponding to the band gap state reveals that electrons are localized around the  $V_O$  site (Fig. 4), forming a deep level trap state. The charged traps by electrons or holes will cause the reliability degradation. The localized state of  $V_O$  in  $ZrO_2$  is also in the band gap but close to the conduction band (CB). The calculated  $E_f^v$  are 5.76 eV and 6.11 eV for  $HfO_2$  and  $ZrO_2$  respectively, consistent with other publications [8, 9].

In the Al-doped  $HfO_2$ , the deep trap level is shifted upward to a shallow level, as shown in Fig. 3. In contrast to this, the deep trap level still remains near the mid-gap in the La-doped  $HfO_2$ . Since deep level states more easily trap electrons or holes than shallow level, Al- and La-doping  $HfO_2$  can cause different reliability characteristics [11].

Figures 5 and 6 show that  $E_f^v$  is remarkably reduced by 2 eV in Al- or La-doped  $HfO_2$  or  $ZrO_2$ , while slightly reduced in

the Ti-doped counterparts. This could be owed to major physical origin for the significant decrease of forming voltage in Al doped HfO<sub>2</sub> RRAM [12], as the forming process is interpreted to be equivalent to the dielectric soft breakdown accompanying with creation of  $V_O$ . The decrease of  $E_f^v$  can be explained based on the effects of Coulomb interactions and lattice relaxation. Trivalent Al or La ion replacing tetravalent Hf or Zr ion forms an acceptor in HfO<sub>2</sub> or ZrO<sub>2</sub> [6].

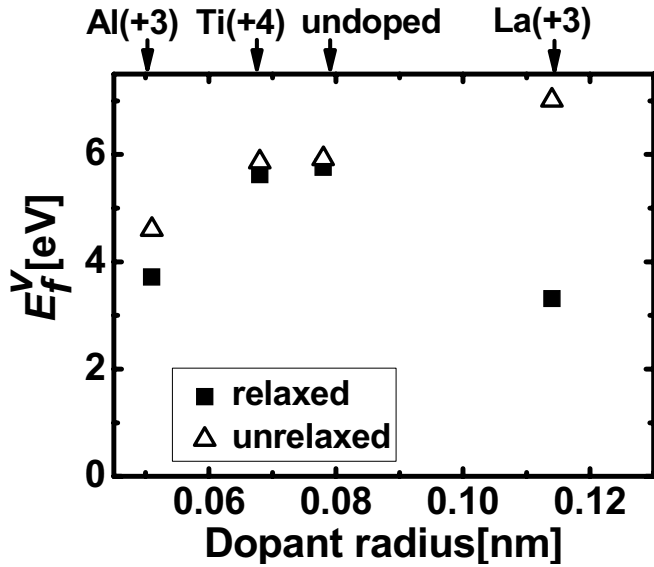


Fig5. The relaxed and unrelaxed  $V_O$  formation energy of doped and undoped HfO<sub>2</sub>. Trivalent ions significantly reduce the relaxed  $E_f^v$ . The unrelaxed  $E_f^v$  is increased with the dopant radius.

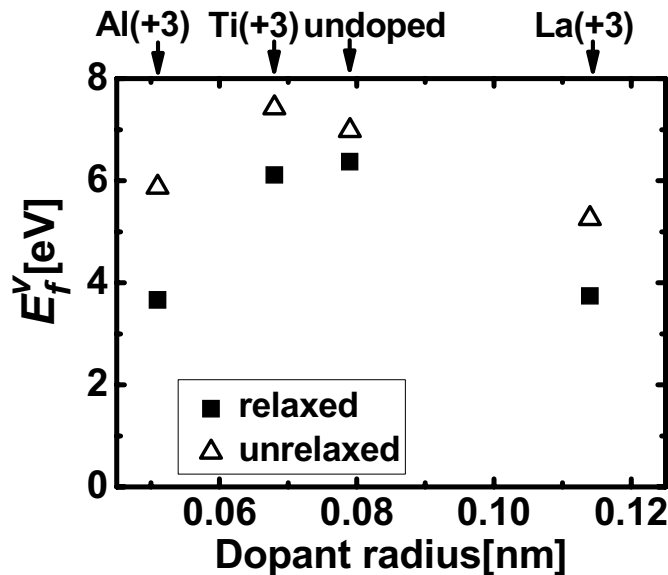


Fig6. The relaxed and unrelaxed  $V_O$  formation energy of doped and undoped ZrO<sub>2</sub>. Trivalent ions reduce the  $E_f^v$  significantly. The unrelaxed  $E_f^v$  is also reduced by the trivalent dopant.

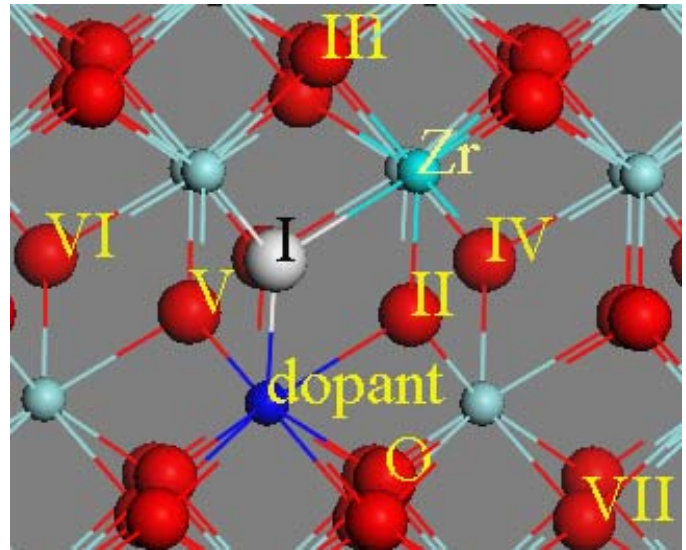


Fig7. Different oxygen sites in the monoclinic ZrO<sub>2</sub> corresponding to possible  $V_O$  sites (white), labeled by capital letters.  $V_O$  can be separated or be NN to the dopant.

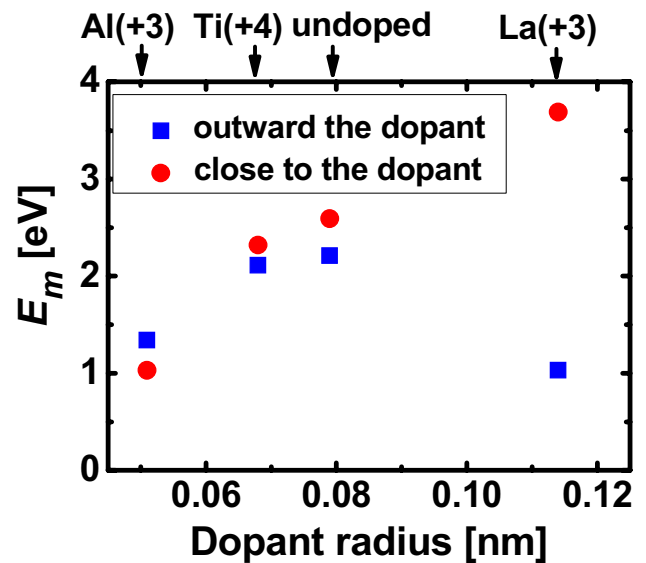


Fig8. The migration barrier ( $E_m$ ) for  $V_O$  or oxygen to migrate close to the dopant and the minimum  $E_m$  for  $V_O$  to migrate outward to the dopant (migration path from I to III in Fig7).

The localized electrons in the  $V_O$  site can be excited and delocalized, leading to the  $V_O$  being positively charged. Therefore, the negatively charged trivalent ion (as the ionized acceptor) will tend to combine with the positively charged  $V_O$  (as the ionized donor), resulting in decrease of the total energy. This is consistent with the decrease of unrelaxed  $E_f^v$  in Al-doped HfO<sub>2</sub> and ZrO<sub>2</sub> and La-doped ZrO<sub>2</sub>. In addition to this, dopant with smaller ion radius (like Ti) benefits the lattice relaxation when the vacancy is formed. From analysis of DOS of HfO<sub>2</sub> with  $V_O$ , the localized electrons will partly occupy the 5d states of Hf atoms, leading to the neighboring

Hf<sup>4+</sup> transforming into Hf<sup>3+</sup> ions, with ion radius increased. In ZrO<sub>2</sub>, similarly in HfO<sub>2</sub>, when V<sub>O</sub> is formed, the neighboring Zr<sup>4+</sup> will also transform into Zr<sup>3+</sup>. This will cause the lattice distortion. Doping of smaller radius ions than Hf and Zr like Ti and Al causes the decrease of the energetic cost of these distortions. This can account for the decrease of E<sub>f</sub><sup>v</sup> in Ti-doped HfO<sub>2</sub>. We also notice that the unrelaxed E<sub>f</sub><sup>v</sup> in La-doped HfO<sub>2</sub> is increased while the relaxed E<sub>f</sub><sup>v</sup> is decreased compared to the undoped HfO<sub>2</sub>. The relaxation energy is more than 3 eV. The large relaxation energy is due to the different structures between La<sub>2</sub>O<sub>3</sub> and HfO<sub>2</sub>, in which the coordination number of cation is different.

The E<sub>m</sub> with different migration paths of V<sub>O</sub> in ZrO<sub>2</sub> is evaluated, considering the unequivalence of the three coordinated V<sub>O</sub> and four coordinated V<sub>O</sub> in monoclinic ZrO<sub>2</sub>. Figure 7 shows the different locations of V<sub>O</sub> with respect to the dopant. V<sub>O</sub> can be NN to the dopant or be separated from the dopant. The migration of V<sub>O</sub> (equivalent to the oxygen moving in the opposite direction) can thus be classified as migration close to or outward to the dopant. The calculated values of E<sub>m</sub> are presented in Table I with different paths indicated by the initial and final V<sub>O</sub> locations indicated in Fig.7. For migration of V<sub>O</sub> or oxygen close to the dopant, the E<sub>m</sub> increases with dopant radius. It can be explained by the fact that oxygen atom is less favorable to pass through the saddle point near the large cation. In contrast to this, the minimum E<sub>m</sub> for V<sub>O</sub> to migrate outward to the dopant (oxygen to migrate oppositely toward the dopant) decreases when trivalent Al or La is doped, and slightly decreases when Ti is doped, as shown in Fig. 8. This can be attributed to the large lattice relaxation in Al- and La-doped ZrO<sub>2</sub>. The relaxation energy of Al- and La-doped ZrO<sub>2</sub> is larger than that of

Ti-doped and undoped ZrO<sub>2</sub>. Thus, relaxation may facilitate oxygen atom to move in a certain direction. It is also noticed that the migration path with the minimum E<sub>m</sub> is the same for Al-, Ti- and La-doped and undoped ZrO<sub>2</sub>. Therefore, the minimum migration E<sub>m</sub> of V<sub>O</sub> is decreased by Al and La dopant.

### Conclusion

First principles calculations were performed to investigate the doping effects of trivalent (Al or La) or tetravalent metal atoms (Ti) incorporating into HfO<sub>2</sub> or ZrO<sub>2</sub> on the formation energy, DOS, and migration barrier E<sub>m</sub> of V<sub>O</sub>. It has been presented that V<sub>O</sub> formation energy is decreased by doping trivalent Al and La in HfO<sub>2</sub> or ZrO<sub>2</sub>. Al doping also causes the shift of V<sub>O</sub> from the deep trap level to shallow level. Al, Ti, or La doping impacts the migration barriers of V<sub>O</sub> along different directions and the minimum E<sub>m</sub> of V<sub>O</sub> among the migration barriers outward to the dopant is decreased. The calculations will help to understand the physical origins of the ionic doping effects on the V<sub>O</sub> and to seek the effective path to control the device characteristics.

### Reference

- [1]A. Kerber et al. EDL. **24**, 87(2003);
- [2]H.Y. Lee et al. IEDM Tech. Dig. 2008, p297;
- [3]W. Guan et al. EDL. **29**, 434(2008);
- [4]R. Waser et al., Nature Materials, **6**, p833 (2007);
- [5]M. D. Segall et al, J. Phys : Condens. Matter, **14**, p2717 (2002);
- [6]N.Umezawa et al, Appl. Phys. Lett. **93**, 223104(2008) ;
- [7]D. A. Andersson et al, Appl. Phys. Lett **90**, 031909(2007);
- [8]A. S. Foster et al, Phys. Rev. B **64**, 224108(2001);
- [9]W. Chen et al, Appl. Phys. Lett. **89**, 152904(2006);
- [10]M. Balog et al, Thin Solid Films, **41**, 247(1977);
- [11]M. Sato et al. Symp. on VLSI Technol.2008, p66;
- [12]B. Gao et al. Symp. on VLSI Technol. 2009(to be published)

Table I. The migration barrier of oxygen or V<sub>O</sub> between the neighboring sites in ZrO<sub>2</sub>. The capital letters indicate the lattice O sites of the lattice, corresponding to the labels in Fig. 7. N<sub>Zr</sub> denotes the atom number of Zr or dopant facing both the initial and final V<sub>O</sub> sites.

\*minimum E<sub>m</sub> of V<sub>O</sub> migration outward to the dopant (Oxygen toward the dopant).

Vacancy Transition		Migration Path type	N <sub>Zr</sub>	E <sub>m</sub> (eV)			
From	To			Undoped	Ti	La	Al
I	II	Close to the dopant	2	2.59	2.32	3.69	1.03
V	VI	outward dopant	2	3.58	3.26	2.16	1.66
II	IV	outward dopant	1	2.53	2.41	1.61	2.18
I	III	outward dopant*	2	2.21	2.11	1.03	1.34
II	VII	outward dopant	1	2.78	3.10	1.82	3.26